2
10/4/77

MASTER

UCID- 17426-77-5, 6, 7

Lawrence Livermore Laboratory

Lithium-Water-Air Battery Project: Progress During the Months of May-July

John F. Cooper, Pamela K. Hosmer, and Oscar Krikorian

August 16, 1977

Prepared for U.S. Energy Research & Development Administration under contract No. W-7405-Eng-48.

DISCLAIMER

Abstract

This report summarizes progress made during the work period May-July, 1977.

A report has been published by these authors which outlines the potential role of metal/air fuel cells in automotive transportation. An abstract of the report is included. The energy and dollar cost of metal/air fuel cell systems is estimated, with emphasis given to the energy and dollar cost of aluminum production. Only aluminum, lithium, and (possibly) calcium are capable of providing the power for a full-performance electric vehicle, while aluminum is most favorable from the standpoint of economics.

The electrochemistry of the calcium electrode appears to be similar to that of lithium, although the use of an aggressive anion (chloride) is necessary to prevent rapid passivation of the anode. Faradaic efficiencies were found to approach 100% close to the diffusion-limited dissolution conditions, as in the case of lithium. However, electrode polarizations of about 1.5 V under such conditions would produce an energy efficiency of discharge of about 40%. Future research is aimed at reducing electrode polarization.

The two-stage electrolysis process, proposed by LLL for the efficient production of lithium, was subjected to further experimental verification. Faradaic efficiencies exceeding 95% were obtained for the formation of Li(Hg) from aqueous LiOH at temperatures up to 56°C at 75 mA/cm^2. Concentrations of Li in Hg were obtained which exceeded the liquidus solubility limit by a factor of four without serious loss of efficiency. The solubility of mercury in the candidate fused salt was determined and found to be acceptably low: 250 ppm.

1. Introduction

Progress has been made these past three months in the three major areas:

(1) High performance metal/air fuel cells have been reviewed with emphasis on their potential role as electric vehicle power sources. Detailed estimates have been made on: (a) performance capabilities and limitations (State of Art and projected); (b) total cost of the fuel cell, and that of support infrastructure for the metal fuel production, distribution, service station handling, and recycling; (b) total energy balance in terms of the quantity of coal consumed by the alternative routes of metal (e.g., Al) production and syncrude/gasoline production. In this study, emphasis is placed on the current costs (dollar and energy) of the domestic aluminum industry and on the experience of Compagnie Générale d'Electricité with the Zn/air cell.

(2) The electrochemistry of the anodic dissolution of calcium has been investigated in mixed alkaline/chloride, aqueous-based electrolytes. Polarization and Faradaic efficiency data have been obtained indicating the potential for a calcium/air fuel cell with about 40% energy efficiency of discharge. Improvements on this performance level are now being sought through alloying, electrolyte additives, changes in the supporting electrolyte, and through control of system hydrodynamics.

(3) Two critical questions have been favorably resolved concerning the lithium production concept under development at this laboratory. (This process yields lithium from a feedstock of a water-soluble lithium compound by means of a two-stage electrolysis involving the intermediate production of a Li(Hg) amalgam). (a) Lithium amalgams have been produced by the electrolysis of concentrated LiOH solutions at temperatures up to 56°C and at Faradaic efficiencies above 95%; the amalgam concentration was found to exceed the solubility of lithium in the liquidus phase by a factor of 4 without loss of efficiency. (b) The solubility of mercury in the fused salt at 300°C was found to be acceptably low: maximum of 260 $\pm$ 250 ppm.

2. High Performance Metal/Air Fuel Cells

A paper of this title has been released.[1] Part I is a general review of the metal/air systems, with emphasis on the current state of their development and feasibility of their use in terms of energy and economics. The abstract is given below. Part II presents basic electrochemical data on the various systems (including those studied at this laborabtory); it is published in a separate volume in order to include patentable or proprietary information.

Abstract Metal/air fuel cells are reviewed in terms of their potential application in electric vehicles. Attention is focused on those metals (light alkali and alkaline earth metals, and aluminum) which, in combination with oxygen, have theoretical energy densities (2-13 kWh/kg-metal) exceeding that of gasoline (utilized in automobiles at 2-3 kWh/kg). Lithium and aluminum have yielded 8- and 4 kWh/kg, respectively, in laboratory experimental cells. The slurry Zn/air system achieves 0.85 kWh/kg-Zn in prototype vehicle cells and is reviewed for comparison. Calcium can probably yield 1.8 kWh/kg-Ca, but its potential as a fuel has not yet been fully explored. The remaining metals appear to be unsuitable for use in aqueous electrolyte fuel cells.

The discharge characteristics of lithium, aluminum, and (possibly) calcium/air cells indicate the potential for (1) electric vehicles of the highway performance and minimum range (300 miles) of subcompact automobiles; (2) rapid refueling for unlimited range extension; and (3) the storage in the fuel cell of sufficient metal for ranges in excess of 1000 miles. Barriers to the concept are the economic necessity of recycling cell reaction products (except in the case of calcium), the expansion or creation of vast metal production industries, and the change-over of existing service station infrastructures to allow electric vehicle servicing.

The energy efficiency of a transporation system using aluminum was estimated using data on the current aluminum production industry. The total (coal to road-load) energy conversion efficiency is roughly 7-9% -- comparable to that projected for the use of synthesized gasoline (H-Coal process) in an internal combustion engine. The efficiency of aluminum production is likely to improve in the future.

An estimate of the cost of fuel cell ownership and operation is derived, relying heavily on the current selling price of aluminum and lithium, and on the performance and projected cost of the C.G.E. air cathode.* At $1.06/kg-Al, the cost of aluminum production makes the greatest contribution (65%) to the total estimated cost of ownership and operation of an aluminum/air cell: 3.0-3.6¢/km, assuming 5.5 kWh/kg-Al utilization. Cost of fuels transportation and handling are below 10% of the total cost.

---

*C.G.E., Compagnie Générale d'Electricité; Marcoussis, France.

The hypothetical introduction in 1985 of one-million electric vehicles using aluminum would require an expansion of the domestic production by about 4% (cf., 8%/y average for the last decade). On the other hand, no comparably sized industries for lithium or calcium production exist -- a formidible barrier to the use of these metals in the intermediate term.

The relative rarity of lithium would complicate the recycling process by necessitating low materials losses per cycle. The availability of lithium ore resources is also potentially a problem. In contrast, the extreme abundance of calcium suggest a potentially important role for this metal, should it prove suitable for use in an aqueous electrolyte fuel cell.

(Editor's note: a sample of thealloy, NUSCAL Alloy MRLA-6, has been obtained from Lockheed Missiles and Space Company; we intend to determine anode polarization and Faradaic efficiency under well-defined conditions of hydrodynamics, current density, temperature, and electrolyte composition. The alloy has yielded the polarization curve shown in Figure (1)).

3. The Anodic Dissolution of Calcium in Aqueous Electrolytes

We are currently surveying the behavior of the calcium electrode in mixed halide-hydroxide electrolytes. The combination of sodium hydroxide and sodium chloride was chosen as a model in anticipation that these two electrolytes alone would produce the extremes of passive and active behavior respectively. With a combination of these we hoped to produce a higher Faradaic efficiency and lower polarization than afforded by either electrolyte when used alone. The electrode behavior is conveniently expressed in terms of Faradaic and voltage efficiencies, or their product--energy efficiency.

The Faradaic (or Coulombic) efficiency may be defined for the calcium anode as the ratio of the equivalents of charge delivered to the external circuit to the equivalents of metal dissolved. It may be calculated from the total volume of hydrogen evolved using the following equation:

$$e_F = \frac{It/2F}{PV/RT}$$

where I is the current applied to the cell; t = dissolution interval; F = Faraday constant; P = partial pressure of hydrogen; V = volume of hydrogen evolved; R = gas constant, and T = absolute temperature.

Voltage efficiency is meaningful only when related to a net cell reaction. For our purposes the half-cell polarization data for the calcium electrode is converted to a voltage efficiency of a calcium/air cell using the following equation:

$$e_V = (3.42 - 0.4 - 3.27 - E_{Ca/SCE}) / 3.42$$

where 3.42 is the theoretical voltage of the calcium/oxygen couple; 0.4 is the polarization (at 0.1 A/cm^2) of a typical air cathode used in alkaline electrolytes; -3.27 is the electrode potential (theoretical) of the $Ca(OH)_2$ electrode (V vs. SCE); and $E_{Ca/SCE}$ is the experimental potential of the calcium electrode measured with the use of a saturated calomel reference electrode.

Electrode potential and Faradaic efficiency were measured simultaneously with the use of an electrolysis cell contained in a sealed vessel. The anodes were disks of calcium metal embedded in epoxy holders. The anodes were approximately of 1-cm^2 surface area. Hydrogen evolution rates were measured from the volume of electrolyte displaced from the cell into a graduated pipette. Appropriate corrections were made for the vapor pressure of water above the electrolyte. Electrolyte convection was provided by a magnetic stirring bar.

In Figure 2, the approximate regions of distinct electrode behavior are shown on a composition map. High and low ration of hydroxy - to-chloride concentration produced the extreme behavior of rapid passivation and rapid corrosion. An intermediate concentration range produced an electrode polarization behavior (upon current scan) similar to that of lithium: a low potential, linear polarization region was followed by a rapid rise in polarization (i.e., passivation) above a critical current density.

Figure 3 shows sample electrode polarization curves, which are typical of the various composition regions. The polarization behavior was time-dependent in the "Critical current passivation" region, and the polarization at a constant current decreased with time. A similar effect had been observed with lithium dissolution ("transient passivation").

Voltage efficiency showed an inverse dependence on Faradaic efficiency as shown in Figure 4a. Faradaic efficiencies of up to 100% were obtained, although at a loss of cell voltage. The highest energy efficiencies were obtained for compositions within the critical current passivation region, near the limiting concentration. The highest energy efficiency was approximately 40%.

In these initial experiments, designed to survey the electrochemical behavior of calcium, relatively impure "off-the-shelf" calcium was used. The composition was determined by emission spectroscopy and shown in Table I. A sample of higher purity was obtained and will be evaluated during the next work interval.

4. The Recyling of Lithium: Experimental Study of the Lithium Amalgam Electrode in Aqueous Electrolyte

The lithium production concept under development at LLL has been described in detail elsewhere.[4] In summary, the process employs a lithium amalgam electrode which circulates continuously between an aqueous electrolysis cell (where it is formed) and a fused-salt cell (where the amalgam is electrolytically refined to a pure lithium melt. The electrochemical behavior (polarization and Faradaic efficiency) of the Li(Hg)/aq.-LiOH and the Li(Hg)/fused-salt electrodes are under investigation.

The aqueous cell electrode was investigated by L.L.L. Summer Institute Fellow, Professor Jeffrey James (Savannah State College, Georgia).[5] The experimental cell is a closed system operating at constant temperature and atmospheric pressure and is described by the following:

$$O_2(Ni)/\ 5.1\ M\ LiOH\ /\ Li(Hg),\quad T = 21\text{-}56^\circ C$$

Electrolyte convection was provided with the use of a magnetic stirring bar encased in lucite. Electrode potentials were measured with the use of Luggin capillary and a Hg/HgO, 5.1M LiOH reference electrode at the same temperature. Faradaic efficiency was determined from the volume of gas evolved (at constant temperature and pressure), with corrections for the vapor pressure (P_{H_2O}) of the electrolyte, using the following equation:

$$\text{efficiency} = \frac{\text{equivalents of Li(Hg) produced}}{\text{equivalents of charge passed}}$$
$$= 1.500 - 2F(P-P_{H_2O})(dV/dt)/(RTI)^*$$

where F is the Faraday constant; P, atmospheric pressure; dV/dt, volume rate of gas evolution from anode and cathode; R, gas constant; T, absolute temperature; and I is the applied current (galvanostatic). Current was varied from 20- to over 100 mA/cm^2. In each determination, the electrolysis began with a fresh mercury cathode, and lithium concentration determined by integration of the efficiency vs. charge-passed curves.

There are several important conclusions to be derived from this work. First, as shown in Figure 5, the Faradaic efficiency tends to increase with current density at a fixed amalgam concentration. Secondly, the

*In reference (4), the efficiency equation was in error; the efficiencies correctly calculated from the earlier data are presented in Figure 5 of this report.

amalgam concentration corresponding to saturation of the liquidus phase (occuring 1.33 at % at 25°C)[5] may be exceeded without serious loss of Faradaic efficiency, up to a factor of about 4. Finally, as shown in Table II, the same behavior obtains up to temperatures of at least 56°C. However, the maximum concentration for efficiencies in excess of 90% falls off with increasing temperature. Apparently, continued deposition of lithium into mercury above the saturation level leads to either a metastable supersaturation, or, more likely, to the formation of a dispersed solid phase, consisting of an intermetallic compound.

5. The Recycling of Lithium: Experimental Study of the Compatibility of the Candidate Fused Salt with Mercury at Operating Temperatures.

The proposed technique for lithium production calls for the electrolysis of a lithium-mercury amalgam in a fused salt cell at a temperature in the range of about 190-260°C. A series of candidate fused salts were developed for use in this cell, containing mixtures of lithium and potassium halides. A major unknown has been the solubility of mercury in the fused salts at operating temperatures. In order to determine the solubility, mercury and a salt mixture of the composition shown in Table III were added to a molybdenum crucible and heated to 300°C. After freezing the mixture, the salt was removed and analyzed by X-ray Fluorescence Spectroscopy. The concentration of mercury was found (by aliquot addition technique) to be 260 ± 250 ppm Hg--i.e., very close to the lower limit of detection. It is concluded that mercury solution and diffusion to the lithium electrode will not be significant. (Note that the transport of uncharged mercury in the fused salt is diffusion-limited; at these concentration levels, the transport rate of Hg is orders of magnitude below that of Li+ across the interelectrode gap.)

Table I. Composition of Calcium Electrodes (ppm by weight)

	Alfa Chemical Company**	Y-12 Purified Sample
Mg	3000	2000
Sr	800	(not reported)
Si	100	< 5
Ba	30	(not reported)
Fe	30	<25
Mn	30	<25
Al	20	< 5
Cu	3	< 5
Na	< 100*	< 5
O	~1%	0.22%

* not detected

** Also not detected (in concentrations below 30 ppm) were B, Cd, Nb, Sb, Pb, Zn; below 10 ppm were Mo, Sn, Ti, V, Zr; below 3 ppm, Bi, Co, Ni, Ag, Be, Cr.

TABLE II. SELECTED FARADAIC EFFICIENCY DATA AT VARIOUS TEMPERATURES

Cell: O_2(Ni) / 5.1 M LiOH / Li (Hg)

well-stirred electrolyte and amalgam

galvanostatic current

Temperature (°C)	Current Density (mA/cm^2)	Li Conc. (%-at.)	Amalgam Electrode Potential (V vs. Hg/HgO, 5.1 M LiOH)	Faradaic Efficiency (%)
21	67	0.8	-2.76	100
		1.6	-2.96	100
		3.9	-2.92	96
		5.3	-2.79	95
35	75	0.4	-2.41	99
		1.1	-2.43	94
		2.6	-2.46	94
		3.4	-2.36	89
44	75	1.3	-2.54	95
		2.4	-2.55	92
		3.4	-2.54	86
		3.7	-2.13	84
56	75	0.30	-2.27	95
		0.79	-2.31	90
		1.3	-2.31	82

TABLE III. COMPOSITION OF FUSED SALT TESTED FOR MERCURY SOLUBILITY*

Composition of Intitial Mixture

	Weight	At.%
LiCl	2	10%
KI	29	48
LiI	25 g	42
Total:	56 g	100%

Mercury Content in the Final Mixture 260 ± 250 ppm (wt.) Hg.

*130 g Hg held in contact with fused mixture for 0.25 h at 300°C; then cooled at 3°C/min; mixture froze at 260°C. The solid state phase was analyzed for total mercury content (dispersed and dissolved); the analyzed sample thus reflects the solubility of mercury at approximately the freezing point.

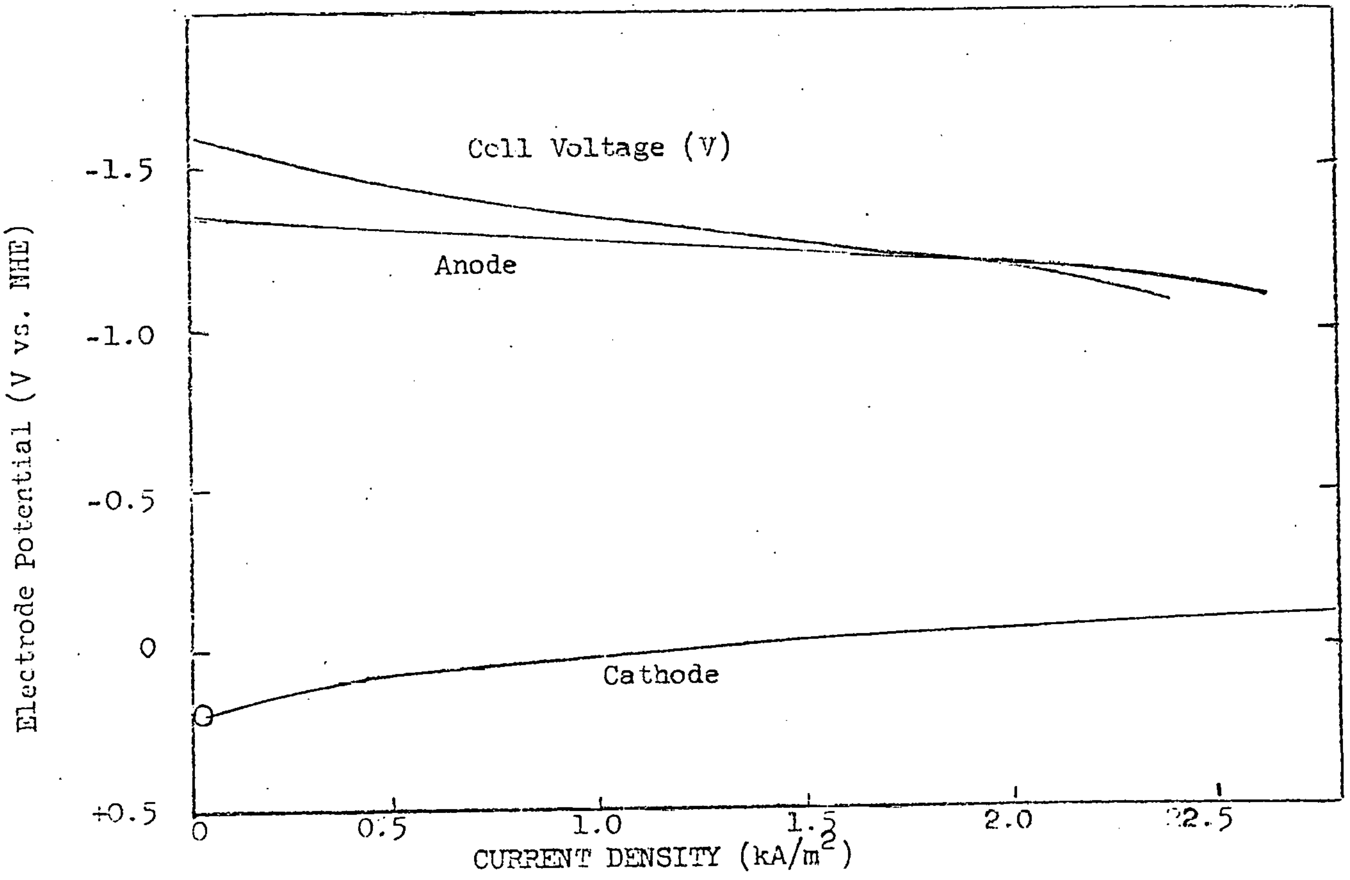

Figure 1. Electrode Polarization Characteristics of Experimental Al/air Cell. Al/ 6M KOH, 0.05 M $Na_2Sn(OH)_6$ / Air-cathode (Pt-catalyzed). Ambient temperature flowing electrolyte. Data from Lockheed Missiles and Space Company.[2] Aluminum alloy is NUSCAL MRLA-6.

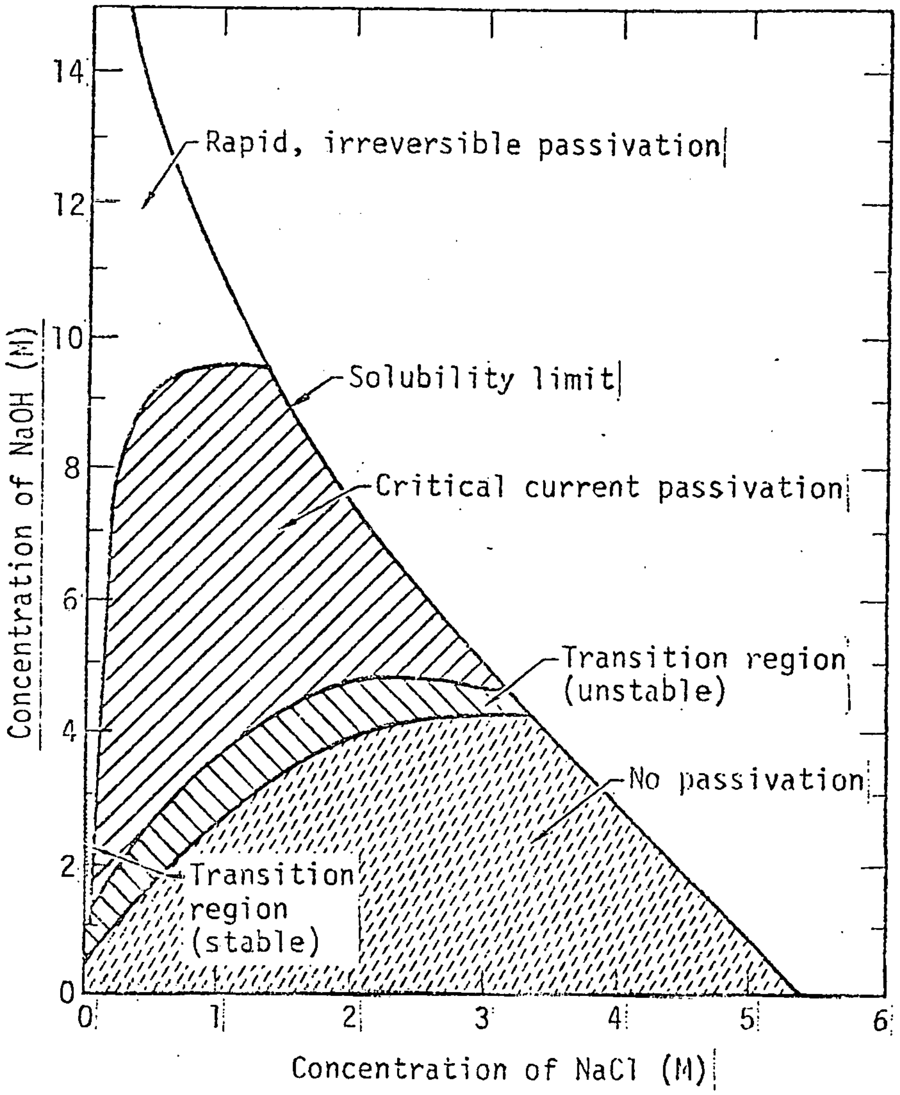

Figure 2. Regions of Distinct Electrode Polarization Behavior of the Calcium Anode. In regions marked "Critical Current Passivation" and "Stable Transition," anode polarization curves show low potential linear polarization region followed by passivation above a critical current density. In region marked" No passivation," no active-passive transition was noted up to current densities of 4 KA/m^2. Highest energy efficiency was obtained near the solubility limit in "Critical Current Passivation" region.

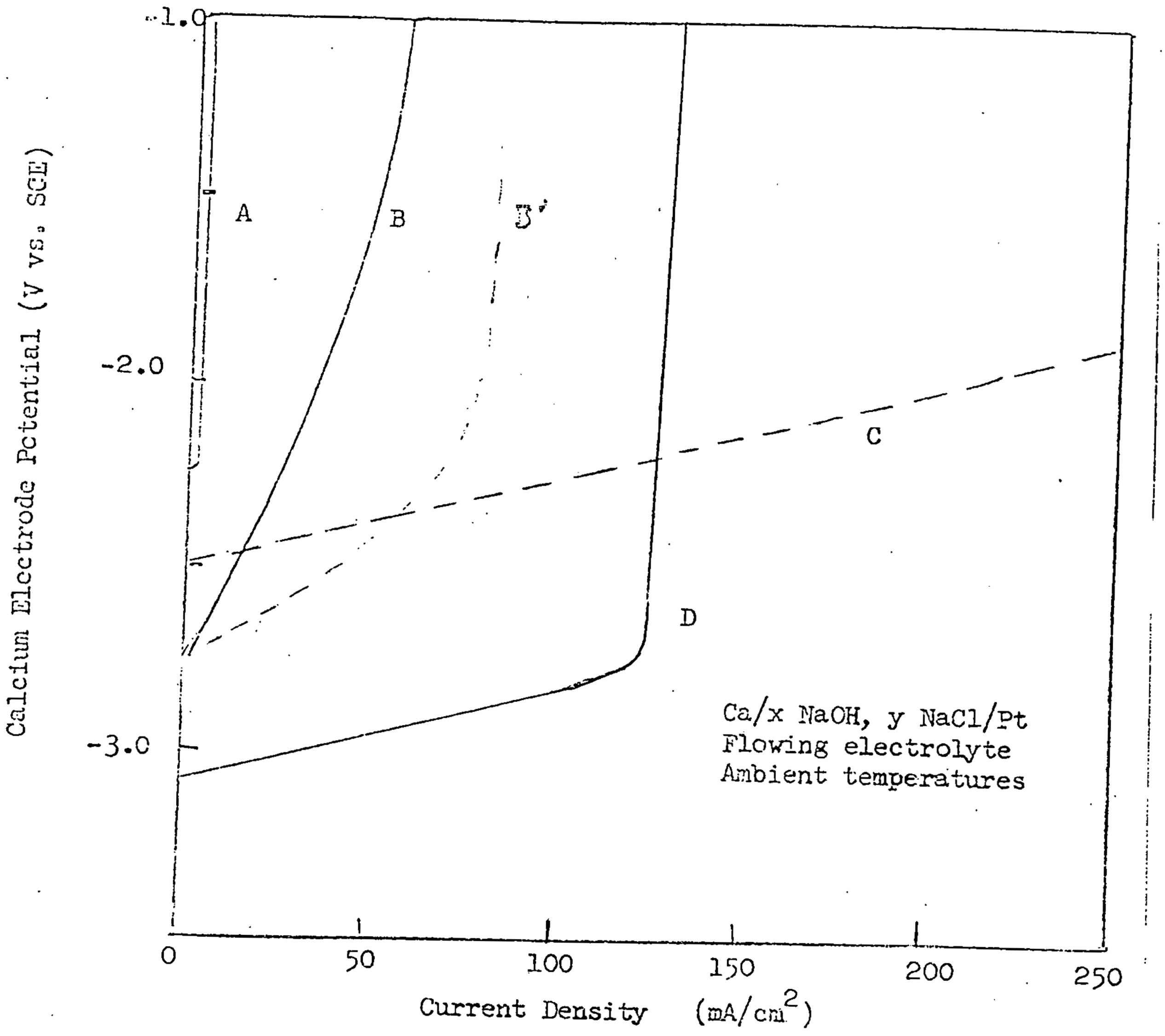

Figure 3. Sample Polarization Curves taken from different Regions of the Composition Diagram (Fig. 2). A. Rapid Irreversible Passivation; B. Critical Current Passivation (slope and limit depend on flow rate); C. No Passivation; D. Stable Transition region.

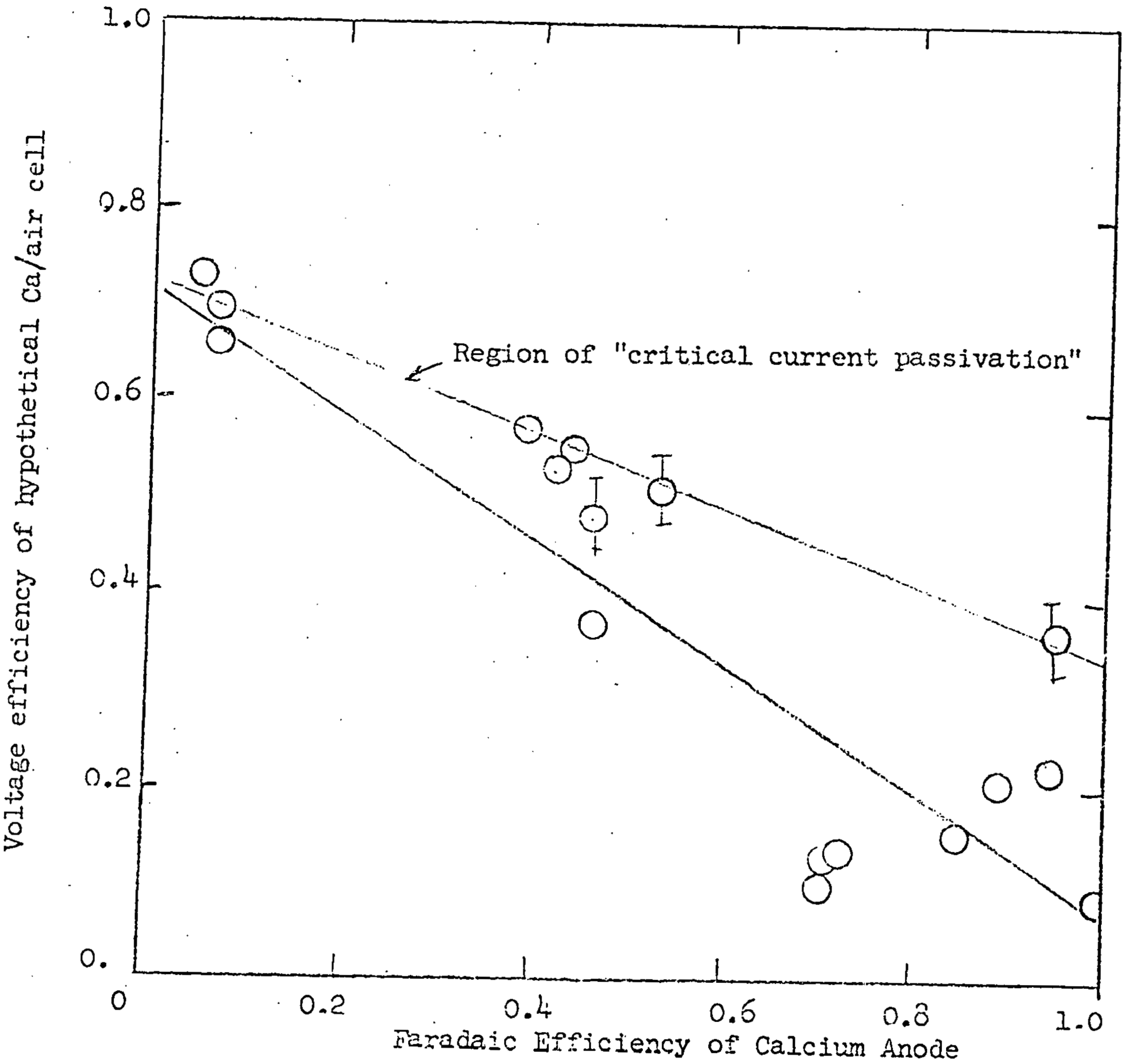

Figure 4a. Relationship Between Voltage and Faradaic Efficiency for Calcium Dissolution. Voltage efficiency is calculated from equation (1) in the text. Highest efficiencies to date obtained in the "Critical Current Passivation" region near to the solubility limit.

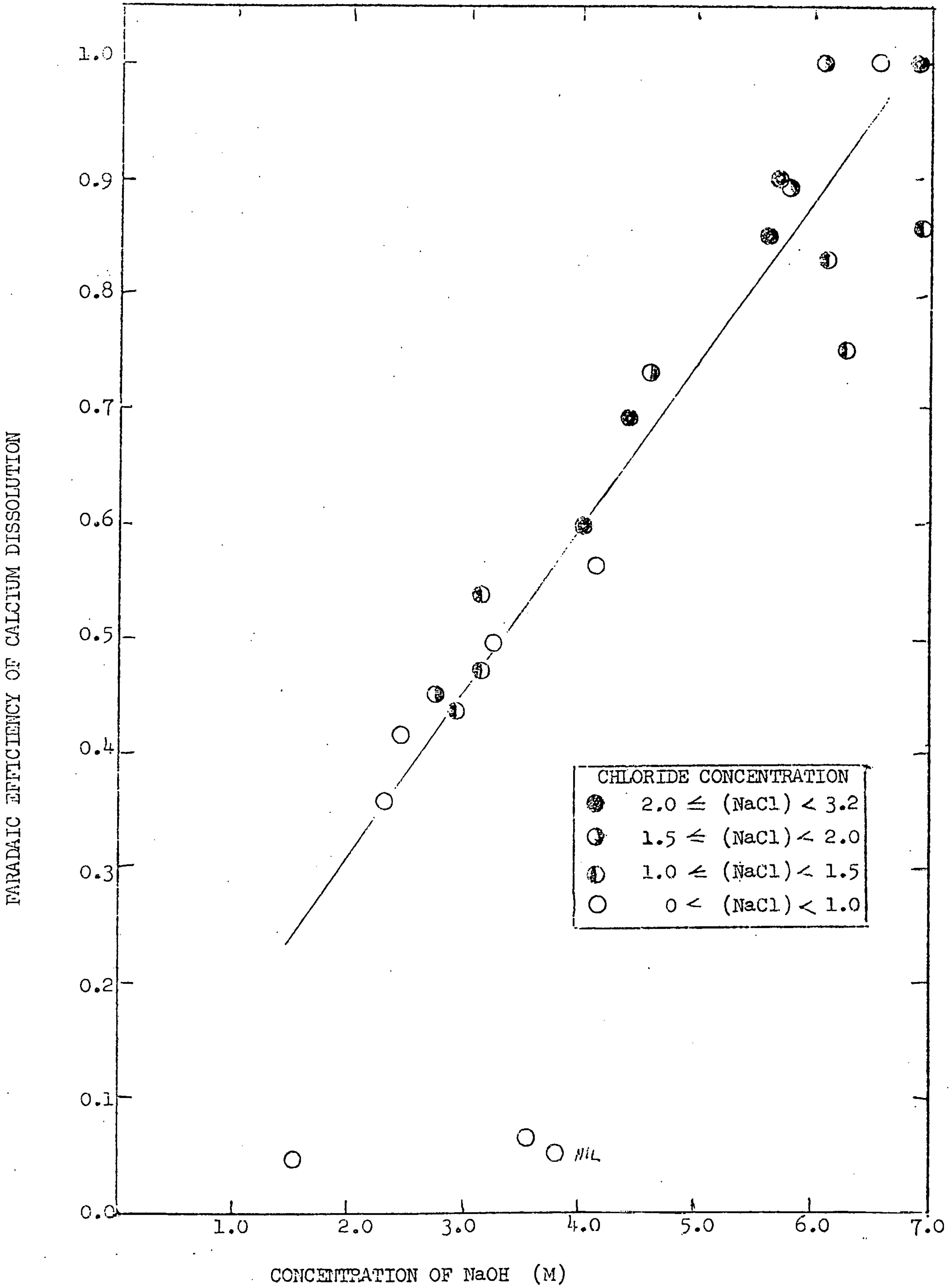

Figure 4b. Dependence of Faradaic Efficiency on Hydroxyl Concentration. System: Ca/ NaOH, NaCl, H_2O/Ni; ambient temperature, stirred electrolyte.

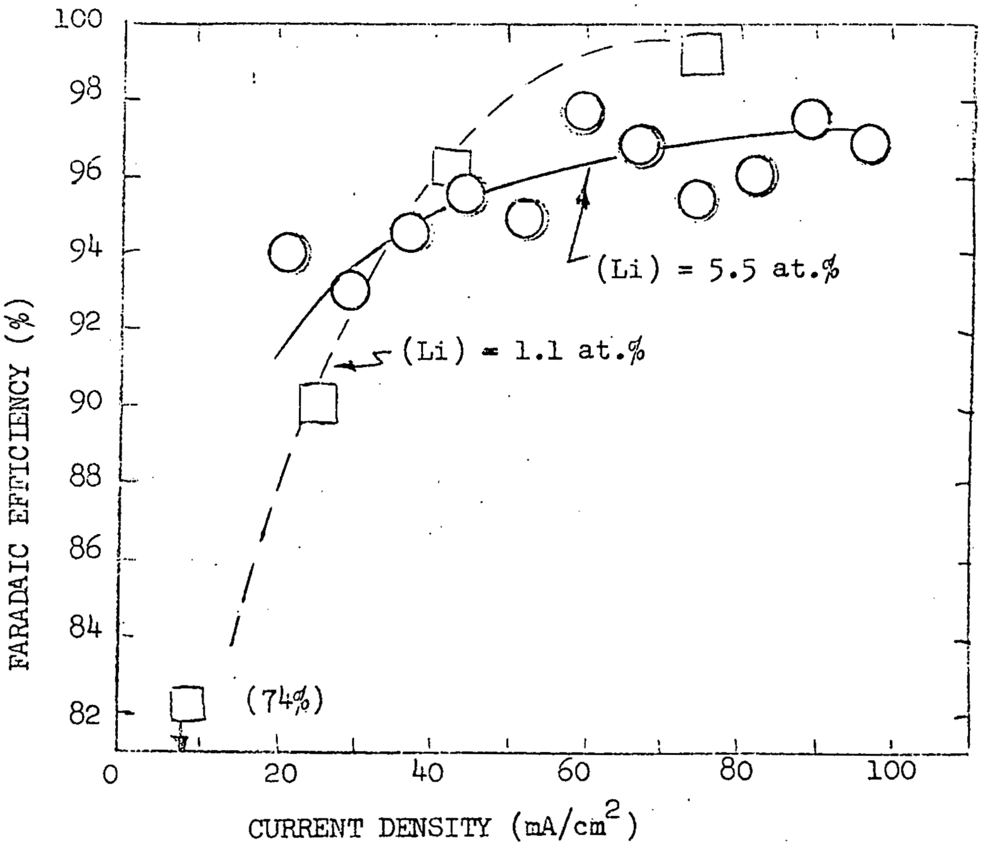

Figure 5. Faradaic Efficiency of Electrodeposition of Lithium Into Mercury at 21°C. Lithium concentration in amalgam: 1.1 ± 0.1 at.%, □ ; 5.5 ± 0.2 at. %, ○. Cell description, O_2(Ni)/ 5.1 M LiOH / Li(Hg); well-stirred electrolyte and amalgam.

References:

1. John F. Cooper, "High Performance Metal/Air Fuel Cells: Part I - General Review," Lawrence Livermore Laboratory, UCID-17558; August 15, 1977; see also Part II - Electrochemical Data.
2. __________, "Follow-on Proposal for the Development of the Lithium-Water-Air Battery for Automotive Propulsion," Lockheed Missiles and Space Company, Palo Alto, C.; LMSC-D084831; June 8, 1977.
3. John F. Cooper and Pamela K. Hosmer, "The Behavior of the Calcium Electrode in Aqueous Electrolytes," paper to be presented to the 152nd Meeting of the Electrochemical Society, Atlanta, Georgia; October 9-14, 1977.
4. See for example, John F. Cooper, et al., "Lithium-Water-Air Battery Project: Progress During the Month of April 1977," UCID-17426-77-4; May 20, 1977.
5. Jeffrey James, "Summary of Characterization of the $Hg(Li)/_{aq}$ LiOH Electrode," UCID _______, August 11, 1977.
6. D. Cogley and J. Butler, J. Phys. Chem. 72, 1017 (1968).

Technical Information Department
LAWRENCE LIVERMORE LABORATORY
University of California | Livermore, California | 94550